Mapping local defects of extended media using localized structures

F. Pedaci, G. Tissoni,[a] S. Barland,[b] M. Giudici, and J. Tredicce
Institut Non Linéaire de Nice, UMR6618 Université de Nice-CNRS, 1365 Route des Lucioles, 06560 Sophia Antipolis, Valbonne, France

(Received 12 May 2008; accepted 12 August 2008; published online 15 September 2008)

The stable positions of localized structures depend on spatial gradients in the system parameters and on the local defects of the hosting medium. We propose a general method to disclose and visualize the local defects of the medium structure, otherwise not detected. The method is based on the observation of the spatiotemporal behavior of localized structures in the presence of controlled gradients in the experimental parameters. We experimentally show an application of this method in a broad-area semiconductor vertical cavity surface emitting laser with optical injection. The comparison of the experimental results with numerical simulations shows a very good agreement. © *2008 American Institute of Physics*. [DOI: 10.1063/1.2977603]

Localized structures (LSs) in optics[1–4] appear as self-sustained, bistable, and independent local peaks of intensity over a homogeneous background that can be switched on or off individually by a proper local optical perturbation. They are promising candidates for data processing due to their mutual independence and plasticity. In particular, when observed in semiconductor microcavities,[5] their control[6,7] is often aimed at providing all optical functionalities for information technology. In contrast, in this letter, we demonstrate that LSs can be used to reveal even extremely shallow inhomogeneities in the bulk of the nonlinear host medium, without any assumption about their exact nature. Indeed, experimental and numerical results,[5,8] as well as analytical calculations,[9] emphasize the pinning role of local inhomogeneities in the stable positions of LSs. In order to detect inhomogeneities, we build on the neutral mode of LSs. If a system is invariant by translation, each solution (and, in particular, a localized one) has a zero eigenvalue, which is connected to the translational degrees of freedom. Since LSs are stable, all their other eigenvalues have negative real part, and therefore any perturbation will mostly couple to the neutral mode, inducing translation.[3,10] Here, we propose to monitor the motion of LSs under the effects of externally applied gradients. Any deviation of a LS's trajectory from the one imposed by the controlled gradients uncovers an underlying inhomogeneity. Therefore, a complete map of the device's inhomogeneities is given by the preferred areas visited by LSs when motion is imposed across the entire section of the device. The arguments presented in this paper involve cavity solitons (CSs), but we refer to them with the more general LS term since our method does not specifically require the presence of a closed cavity.[11,12]

In semiconductor systems (used in the experiment presented below) many inhomogeneities can arise during the growth or postprocessing stages. For example, dislocations due to lattice parameter mismatch can be easily observed. On the contrary, layer thickness variations in Bragg mirrors (structural waviness and interface roughness[13]) are detectable via Reflection High Energy Electron Diffraction during the growth process, but they become much more difficult to reveal in the bulk of a fully grown structure. Even more so, spatial variations in the concentration of the semiconductor constituents or doping are particularly difficult to diagnose.[14,15] Even if several microscopy techniques can be applied to each separate component of a semiconductor system leading to very precise topography of surfaces (with atomic force microscopy. for example) or to deep knowledge of the crystalline structure of thin samples (with transmission electron microscopy), very few methods actually allow to probe the bulk of a fully grown structure besides basic spatially resolved photoluminescence intensity, which as we shall see is not very efficient at revealing certain inhomogeneitites.

We realize the measurement in a broad-area (250 μm diameter) vertical cavity surface emitting laser (VCSEL). The device is electrically driven above transparency and below laser threshold (amplifying regime) and is optically injected by an infrared (980 nm) tunable master laser (holding beam). In this configuration, CSs can be observed in suitable regions of the parameter space (i.e., bias current, detuning between cavity resonance and injection frequency, and holding beam intensity[8]). The near field of the injected VCSEL output facet is then imaged onto a charge coupled device camera. Details about the experimental setup can be found in Ref. 8.

Motion of the CS along the VCSEL plane can be induced by creating gradients in the transverse dimension of the system,[6,10,16–18] for example, by spatially modulating the phase or intensity profile of the holding beam. In order to control the gradients in these parameters, we insert in the path of the holding beam a Mach–Zender interferometer. The phase profile of each beam in the interferometer is kept as flat as possible at the VCSEL plane. If the interferometer is set such that its two arms have slightly different alignment conditions with respect to the VCSEL, the resulting intensity profile of the holding beam is a fringe pattern. Along the direction perpendicular to the fringe, this pattern is able to confine the CSs due to the intensity gradient; i.e., the CS is trapped in the center of the fringe, where the intensity has a maximum. On the contrary, along each interference fringe the intensity is homogeneous, its gradient can be neglected, and the phase gradient in the total holding beam is always

[a]Permanent address: INFM-CNR, Dipartimento di Fisica e Matematica, Università dell'Insubria, Via Valleggio 11, 22100 Como, Italy.
[b]Electronic mail: stephane.barland@inln.cnrs.fr.

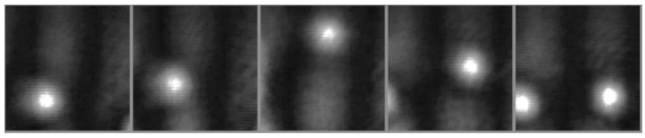

FIG. 1. The CS, adiabatically dragged horizontally, is deviated from the straight trajectory by the inhomogeneity of the medium.

kept to zero. In these conditions, the only mechanisms that can induce a drift of the CS are the (controlled) intensity gradient (in the direction perpendicular to the fringes) and the (unknown) intrinsic gradients of the system (in any direction).

The fringes are then adiabatically shifted horizontally by varying the voltage applied to a piezoelectric mount supporting one of the mirrors in the interferometer. Thus, the CS is expected to follow a straight horizontal trajectory. In contrast, we observe (see Fig. 1) that the CS follows a path going first upwards and then downwards. This deviation has to be attributed to the effect of intrinsic gradients along the vertical direction in the system. We stress that in the absence of any externally imposed confinement along this direction an *arbitrarily small* gradient intrinsic to the system suffices to deviate the motion.

In order to draw a map of the system's intrinsic local gradients, we implement the same procedure on the whole surface of the device. The system is initially prepared such that several CSs are present and distributed in the device. The fringes are then adiabatically shifted, scanning the complete surface in several seconds, infinitely slowly with respect to the semiconductor time scales. This procedure is repeated along the horizontal, vertical, +45°, and −45° directions in the two senses of motion. During the motion of the fringes, CSs will either be repelled or attracted by the inhomogeneities in the device. Therefore, some areas of the device will be visited more, while others will be avoided, providing a map of spatial gradients intrinsic to the system.

A video frame is acquired for each position and orientation of the fringes. Finally, all the frames are added and the resulting image is a gray-scale map of the areas of the plane visited and avoided by CSs. The spatially extended structures present in some regions of the device have been removed by intensity thresholding in each frame in order to eliminate their contribution to the resulting image. The result is shown in Fig. 2 right panel, where black (white) corresponds to high (zero) possibility to host a CS, i.e., to attractive (repulsive) local inhomogeneities. For an ideal defect-free medium, such analysis would result in a homogeneously gray map since the CS stability is identical all across the system. In real systems like the one analyzed here, inhomogeneities appear. Among

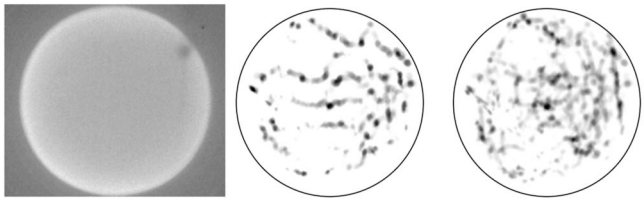

FIG. 2. Left: spontaneous emission profile of the VCSEL. Center: CSs trajectories when dragged toward the left. Right: map of the defects in the VCSEL structure as the result of the complete analysis of the CSs trajectories.

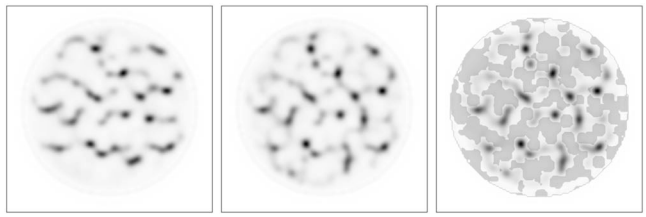

FIG. 3. Left: CSs trajectories in the case of vertical fringes adiabatically shifted toward the left. Center: map of the defects in the VCSEL structure as the result of the analysis of the CSs trajectories. Right: superposition of the map and the surface defined by $\theta(x,y)=-2.0$.

the major defects appearing in Fig. 2, the large white regions at the top left and bottom of the device indicate strong imperfections where CSs cannot be observed or created for these parameter values and the central black spot records, on the contrary, a region of the cavity where a CS is easily switched on. We underline that the spontaneous emission profile of the device (Fig. 2, left) is highly uniform, which suggests rather uniform optoelectronic properties. In contrast, the procedure previously described very clearly puts in evidence the inhomogeneity of the system.

In order to validate our method, we considered a simple rate-equation model already used to predict CSs in semiconductor microcavities[19] and to describe their dynamics.[5,17]

For the aim of accounting for the spatial inhomogeneities related to spatial thickness variations in the layers of the Bragg reflectors, we impose a spatial variation in the cavity detuning parameter, setting $\theta(x,y)=\theta_0+\delta\theta(x,y)$, where $\delta\theta(x,y)$ is a normally distributed stochastic process with zero average and finite spatial correlation length, as in Refs. 5 and 8. The amplitude of the fluctuations depends on the reflectivity and on the distribution of layer jumps associated with the epitaxial deposition, while the correlation length is related to the typical transverse dimensions of the layer defects. Following Refs. 20 and 21 we assumed typical defect sizes on the order of 10–15 μm (diameter). The amplitude of the distribution corresponds to a cavity frequency variation of 60 GHz, i.e., a detuning region larger than the entire CS branch. In this way, we are accounting for strongly "attracting" defects where CSs are easily switched on, as well as for "repulsive" defects where CSs cannot exist.

We prepared the input beam in form of fringes as in the experiment and start the numerical simulation from an initial condition where many CSs are present, preferably at the strong defect locations, that is, where the injected frequency is more blue-detuned with respect to the cavity frequency.[22] Then, we slowly shifted the fringes in a direction perpendicular to their orientation, at a velocity of about 100 μm/μs. This velocity is much larger than in the experiment, but it is small enough to let the system relax to its stationary state (typically, tens of nanosecond).

In Fig. 3, left, we show the CSs trajectories obtained by summing all the frames of the numerical simulation for the case of vertical fringes that are shifted toward the left. The deviation from straight lines is well visible, as it is in the experiment (Fig. 2, central panel).

We repeated the same procedure for different orientations of the fringes (vertical, horizontal, +45°, and −45°) in the two senses of motion. Adding all the frames we obtain a gray-scale map showing the most visited regions of the sample (in black), which correspond to attracting defects, as

well as the avoided zones (in white) (see Fig. 3, center). This map is very similar to the experimental one, but now it can be directly compared with the spatial distribution of defects assumed. The good match between the two (shown on the right panel of Fig. 3) indicates that the sample inhomogeneities modeled as defects in the cavity detuning parameter θ are effectively revealed by our method.

The validity of LSs as a diagnostic tool must be assessed with respect to two criteria, resolution and sensitivity. We note that the local inhomogeneities of the medium cannot be visualized by simply analyzing the emission of the free-running laser (see Fig. 2, left panel) nor by considering spatially extended patterns, since small scale inhomogeneities couple to the whole pattern.[23] LSs, in contrast, are influenced only by the local characteristics of the medium, where "local" roughly corresponds to the spatial extension of a LS. Thus, the spatial resolution of a LS based probe is in this case of the order of 10 μm. The resolution can be improved by working in different parameter regions or systems with smaller LS size. While this is far from state of the art microscopy, the unrivalled strength of this method lies in its sensitivity, and thanks to the existence of the neutral mode of LSs, any gradient, no matter how small, will influence their trajectory, and will therefore be detected. In the simulations we changed the amplitude of the defect distribution and were able to reveal detuning variations of about 2 GHz. The practical limitation comes mostly from the care taken in the preparation of a gradient free holding beam to perform the measurement, with the quality of the optics as the ultimate limiting factor in the homogeneity of said holding beam. Moreover, since LSs are not living on the device surface but are extended in the whole device along the longitudinal dimension, inhomogeneities will be revealed even if they are located in the bulk of the device, independently of their nature, and not only at the accessible surface. No other nondestructive method allows this kind of probing of the bulk of a material. Moreover, we applied the method in a semiconductor microcavity and revealed its inhomogeneities, but it is, in principle, possible to use the same method for revealing the inhomogeneities of any transparent object placed in a compound system able to support LSs such as a liquid crystal light valve with optical feedback. Furthermore, it is in principle possible to precisely determine the parameter gradient that is necessary to overcome the pinning effect of an inhomogeneity. This experiment, which allows an absolute and quantitative measurement of the inhomogeneity, will be published in a future work.

In this letter, we have shown that intrinsic device inhomogeneities can alter the trajectory of LSs when these are subject to controlled parameter gradients. Building on this effect, we have devised and implemented a method based on LSs for probing the homogeneity of the medium, where the sensitivity of LSs to arbitrarily small gradients is turned into their most powerful asset for the detection of imperfect translational invariance.

This work was done in the framework of the FET OPEN (Project No. 4868 FunFACS) (Fundamentals, Functionalities, and Applications of Cavity Solitons). We gratefully acknowledge W. J. Firth for the input at the very origin of the idea of using LSs for mapping local defects. G.T. acknowledges the financial support of the University of Nice. M.G. thanks R. Jäger and J. M. Chauveau for fruitful discussion.

[1] N. N. Rosanov, *Spatial Hysteresis and Optical Patterns* (Springer, Berlin, 2002).
[2] L. Lugiato, IEEE J. Quantum Electron. **39**, 193 (2003).
[3] T. Ackemann and W. J. Firth, *Dissipative Solitons*, Lecture Notes in Physics Vol. 661 (Springer, Berlin, 2005).
[4] P. Coullet, C. Riera, and C. Tresser, Phys. Rev. Lett. **84**, 3069 (2000).
[5] S. Barland, J. R. Tredicce, M. Brambilla, L. A. Lugiato, S. Balle, M. Giudici, T. Maggipinto, L. Spinelli, G. Tissoni, T. Knodl, M. Miller, and R. Jager, Nature (London) **419**, 699 (2002).
[6] F. Pedaci, P. Genevet, S. Barland, M. Giudici, and J. Tredicce, Appl. Phys. Lett. **89**, 221111 (2006).
[7] F. Pedaci, S. Barland, E. Caboche, P. Genevet, M. Giudici, J. R. Tredicce, T. Ackemann, A. J. Scroggie, W. J. Firth, G.-L. Oppo, and G. Tissoni, Appl. Phys. Lett. **92**, 011101 (2008).
[8] X. Hachair, L. Furfaro, J. Javaloyes, M. Giudici, S. Balle, J. Tredicce, G. Tissoni, L. A. Lugiato, M. Brambilla, and T. Maggipinto, Phys. Rev. A **72**, 013815 (2005).
[9] S. Fedorov, D. Michaelis, U. Peschel, C. Etrich, D. V. Skryabin, N. Rosanov, and F. Lederer, Phys. Rev. E **64**, 036610 (2001).
[10] T. Maggipinto, M. Brambilla, G. K. Harkness, and W. J. Firth, Phys. Rev. E **62**, 8726 (2000).
[11] P. L. Ramazza, S. Ducci, S. Boccaletti, and F. T. Arecchi, J. Opt. B: Quantum Semiclassical Opt. **2**, 399 (2000).
[12] M. Pesch, E. Große Westhoff, T. Ackemann, and W. Lange, Phys. Rev. Lett. **95**, 143906 (2005).
[13] M. T. Asom, M. Geva, R. E. Leibenguth, and S. N. G. Chu, Appl. Phys. Lett. **59**, 976 (1991).
[14] J.-S. Kang, G. Kim, S. C. Wi, S. S. Lee, S. Choi, S. Cho, S. W. Han, K. H. Kim, H. J. Song, H. J. Shin, A. Sekiyama, S. Kasai, S. Suga, and B. I. Min, Phys. Rev. Lett. **94**, 147202 (2005).
[15] P. Pohl and R. Brendel, Appl. Phys. Lett. **87**, 032104 (2005).
[16] W. J. Firth and A. J. Scroggie, Phys. Rev. Lett. **76**, 1623 (1996).
[17] L. Spinelli, G. Tissoni, M. Brambilla, F. Prati, and L. A. Lugiato, Phys. Rev. A **58**, 2542 (1998).
[18] U. Bortolozzo and S. Residori, Phys. Rev. Lett. **96**, 037801 (2006).
[19] M. Brambilla, L. A. Lugiato, F. Prati, L. Spinelli, and W. J. Firth, Phys. Rev. Lett. **79**, 2042 (1997).
[20] R. Kuszelewicz, I. Ganne, I. Sagne, G. Slekys, and M. Brambilla, Phys. Rev. Lett. **84**, 6006 (2000).
[21] J. L. Oudar, R. Kuszelewicz, B. Sfez, J. C. Michel, and R. Planel, Opt. Quantum Electron. **24**, S193 (1992).
[22] E. Caboche, P. Genevet, F. Pedaci, S. Barland, M. Giudici, J. Tredicce, G. Tissoni, and L. A. Lugiat (unpublished).
[23] S. Barland, F. Marino, M. Giudici, and S. Balle, Appl. Phys. Lett. **83**, 2303 (2003).